

Study on output pressure prediction and jetting features of ultra-high pressure water jet for the downhole intensifier

Hualin Liao¹, Huajian Wang¹, John-Paul Latham², Jiansheng Xiang²,
Laurent Gerbaud³, Hedi Sellami³

¹China University of Petroleum (East China); ²Imperial College London; ³Centre of Geosciences - MINES ParisTech/ARMINES

Keywords: Downhole intensifier, High pressure water-jet drilling (HPWJ), numerical simulation, jetting features.

ABSTRACT

With the increase of geothermal drilling depth, in-situ stresses increase and are concentrated in the area of action of the drilling bit especially in the peripheral bottom-hole area. This phenomenon increases the yield strength of the rock and reduces its brittleness in drilling performance at greater depth. To increase hard rock drilling rates of deep geothermal reservoirs, a novel drilling technology combining hydro-jet and percussion for rate of penetration improvement is proposed. The innovation lies in developing a new principle to 'free' the rock from these high confining stress concentrations in the local area of mechanical action of the cutters of the drilling bit, only a few millimeters below the bottom of the bore-hole. This will allow the mechanical drilling bit to work in a greatly 'relaxed' and very weakened rock. The most important technology of this new concept is optimization of the hard rock slotting process using a high pressure water jet under the downhole regime of high confining pressures and bottom hole fluid pressures. The downhole intensifiers which could generate high pressure water jets have been applied in field trials which demonstrated a good improvement of ROP. Due to the complex conditions downhole, it is still not known exactly how much jet pressure can be generated in different conditions.

Therefore, the working principle of the intensifier is investigated. The influence of the turbulence model on water jet, the effect of nozzle diameter and WOB were studied based on a CFD simulation. The results show that the results of numerical simulation are greatly affected by turbulence model selection and the RNG k-ε model is used as the turbulence model for jet simulation because of its higher simulation accuracy. With the increase of WOB, the peak nozzle exit velocity and peak pressure are increased significantly. This also increases the time range of the ultra-high-pressure water jet, and furthermore, the increase of the WOB lengthens the holding time of the UHP water jet, and the speed and displacement of the plunger tends to increase. Decreasing the nozzle diameter prolongs the holding time of the high-pressure water jet above a certain threshold value, and the decrease of nozzle diameter makes the pressurization period decrease. In the range of diameters investigated in this research, the smaller nozzle diameter is beneficial to the formation of an ultra-high-pressure water jet. The research can provide a reference for the optimal design of intensifier and will be beneficial for downhole pressurized jet-assisted drilling techniques.

1. INTRODUCTION

Geothermal energy is a kind of clean energy with abundant energy storage and wide distribution. Due to low pollution, renewable, stable production capacity and long service cycle, it has been highly valued by the governments of all countries (Teke et al., 2018). One of the factors affecting the performance of deep drilling operations is linked to the difficulty of breaking deep rock formations with acceptable rate of penetration (ROP). Indeed, when they are subjected to strong geostatic stresses and hydrostatic pressures (Lu et al., 2020).

In order to solve the problem of low ROP, which is caused by high in-situ stress, the novel drilling technology combining hydro-jet and percussion for ROP improvement in deep geothermal drilling is proposed by H2020 EU research project. The innovation lies in developing a new principle to 'free' the rock from these high confining stress concentrations in the local area of mechanical action of the cutters of the drilling bit. This will allow the mechanical drilling bit to work in a greatly 'relaxed' and very weakened rock.

One of the most important technologies in this new concept is the ability to generate ultra-high-pressure water jets. There are essentially two technical means of delivering the pressure: downhole pressurization and ground pressurization (Guan et al., 2012). Maurer increased the mud pressure to 68-105MPa by means of ground pressurization and found that ROP could be increased by 2~3 times (Maurer et al., 1973); the experimental study of the high-pressure drill bit equipment developed by Exxon Company found that increasing the pump power could increase the ROP by 5~8 times (Liao et al., 2005). Although ground pressurization equipment has significantly improved ROP, it has not been widely used because of the complexity and cost of the equipment and the significant impact of the depth of the well (Liao et al., 2015). Downhole pressurization techniques that exploit the driving force of the plunger, can be classified into two types: utilizing the drilling fluid hydraulic power and utilizing axial vibration energy of the drill string. The intensifiers that utilize drilling fluid hydraulic power include many principles and types: hydrostatic (Ai et al., 2001; Sun et al., 2006), diaphragm (Ai et al., 2001), centrifugal style (Sun et al., 2006), screw motor style (Zhao et al., 2010; Xu et al., 2011), jet booster (Wang et al., 2008; Xue et al., 2010; Xue et al., 2012) and so on.

The intensifier type that utilizes the axial vibration energy of drill strings can alleviate cutter collapse, string fatigue damage, and ground equipment damage, and increasing ROP by up to 8 times compared to the same conditions without the intensifier (Guan et al., 2014). Due to the complex conditions downhole, it is still not known exactly how much pressure can be generated in different conditions.

2. WORKING DESCRIPTION OF INTENSIFIER

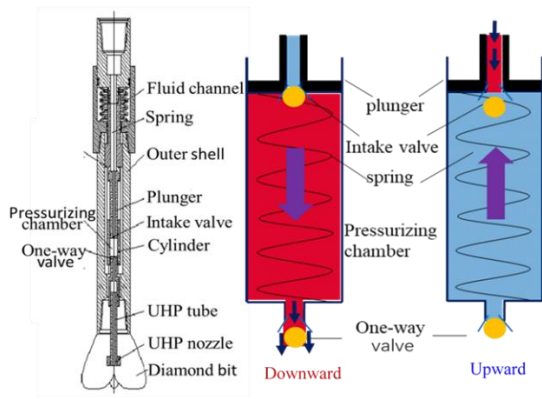


Fig.1 working principle of the intensifier

Figure 1 shows the working principle of the intensifier, for the intensifier that utilizes the axial vibration energy of drill strings. When the axial downward vibration load of the drill string exceeds the pre-tightening force of a spring, which is compressed, a plunger is driven forward within a pressurizing chamber and the intake valve is closed, hence the fluid inside the chamber is pressurized. During the upstroke, due to the effects of the spring and axial vibration of the drill string, the plunger is driven upward, the intake valve is opened and the one way valve is closed, allowing the fluid back into the chamber. The flow of drilling fluid is as shown in figure 2.

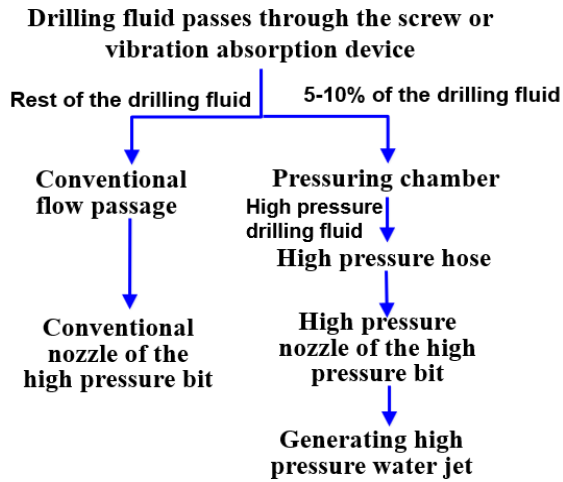
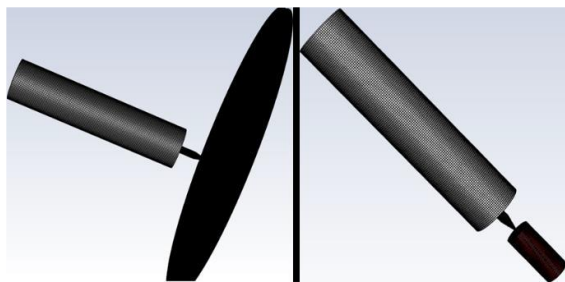


Fig.2 Flow of drilling fluid

3. METHOD OF NUMERICAL SIMULATION

3.1 Model description



(a) Impinging pressure model (b) Jet features model

Fig. 3 Computational domain geometries and meshes

In order to study impinging pressure and jet features of an intensifier with different parameters, the models of jet features and impinging pressure are established, and the computational domain geometry and meshes are as shown in figure 3. In order to improve the accuracy of the calculation model and increase the computation speed the computational domain is divided into 5.0×10^5 hexahedral mesh elements. In the vicinity of the wall and nozzle, the mesh elements are finer than the remainder of the model. The structural parameters are shown in Table 1.

Table 1 Structure parameters of chamber and nozzle

| Structure | Parameter | Value | Unit |
|----------------------|----------------------|-------|------|
| Pressurizing chamber | Diameter of chamber | 46 | mm |
| | Length of chamber | 200 | mm |
| | Diameter of UHP tube | 8 | mm |
| | Length of UHP tube | 10 | mm |
| | Diameter of inlet | 8 | mm |
| nozzle | Diameter of outlet | 2 | mm |
| | Length | 20 | mm |
| | Angle of convergence | 30 | ° |

3.2 Boundary conditions

It is assumed that the chamber is filled with clean water, the velocity of the liquid in the initial position is 0 m/s, and the liquid in the chamber is pure clear water. A “pressure-outlet boundary” condition is used at the nozzle, and this pressure is set to 0 MPa, the solution type is pressure-based and transient. The turbulent flow is described by a k-ε turbulence model. In order to study the influence of the turbulence model, the impinging pressure and jet features with standard k-ε, RNG k-ε and realizable k-ε are compared. The WOB is set to 100 kN ~ 200 kN, and the nozzle diameter is set to 2 mm ~ 2.5 mm.

4. RESULTS AND DISCUSSION

4.1 Influence of turbulence model on water jet

(1) Velocity distribution

Fig.4 compares the velocity distributions along the axial centerline with different turbulence models. The velocity of the three models at the orifice outlet is basically the same, but with the increase of the axial distance, the velocity changes significantly. The standard k-ε model has the smallest potential core, the length of potential core is about 4 mm. The potential core (i.e. jet length with no significant drop off in velocity) of the Realizable model and the RNG k-ε model is basically the same, and the length of potential core is about 7 mm. With the further increase of axial distance, the velocity attenuation of standard k-ε turbulence model is more rapidly. The velocity attenuation of standard k-ε turbulence model gives the slowest velocities. The RNG k-ε model is used as the turbulence model for jet simulation because of its higher simulation accuracy.

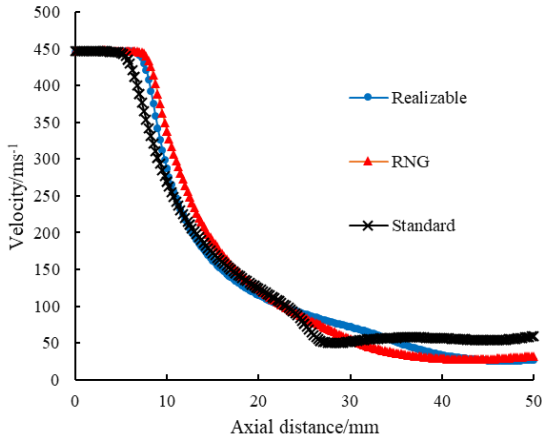
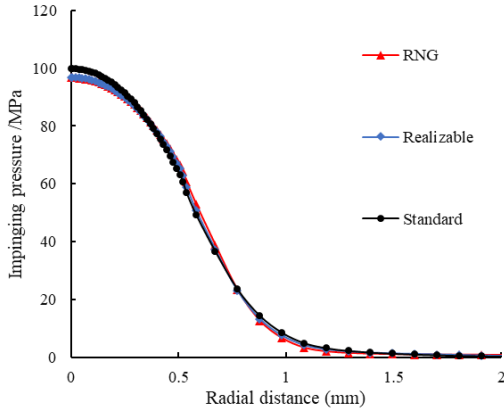


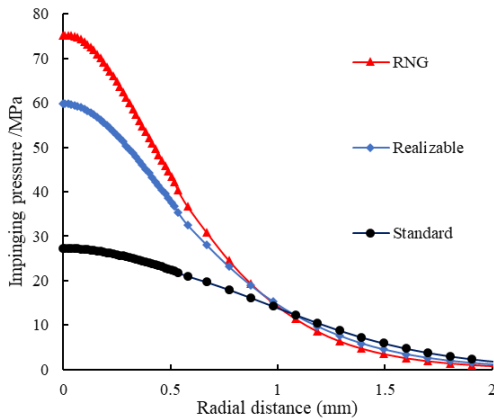
Fig.4 Velocity along axial distance with different turbulence model

(2) Impinging pressure with different turbulence models

Fig.5 compares the impinging pressure with different stand-off distance. When the stand-off distance is 3 mm, the impinging pressure of the three models are basically the same. As the radial distance increases, the impinging pressure decreases gradually, and when the radial distance is 1.5 mm, the impinging pressure decays to 0 MPa. And when the stand-off distance is 10 mm, there are great differences in the distribution of impinging pressure; the RNG model has the maximum impinging pressure, while the standard model has the minimum. This is consistent with the characteristics of velocity attenuation.



(a) Stand-off distance is 3 mm

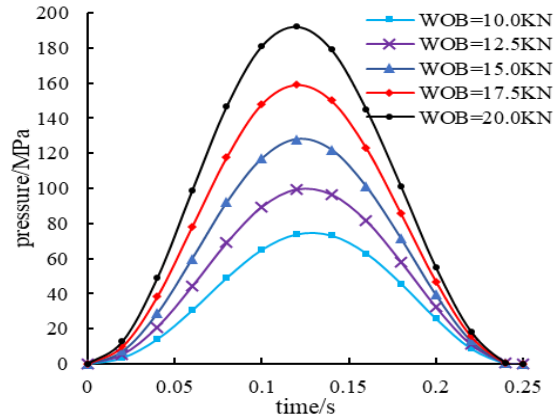


(b) Stand-off distance is 10 mm

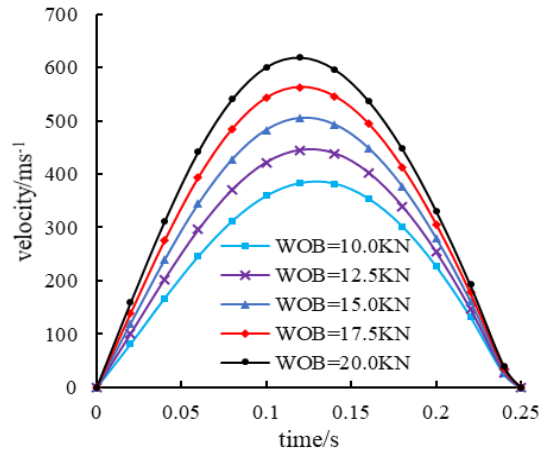
Fig.5 Impinging pressure with different turbulence model

4.2 The effect of WOB

(1) Characteristic of flow field



(a) Pressure of UHP water jet



(b) Velocity of UHP water jet

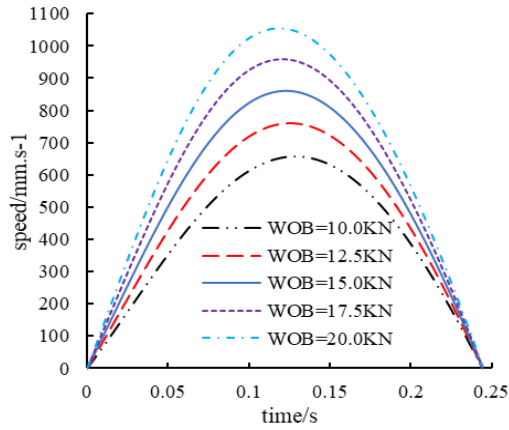
Fig.6 Characteristic of flow field in different WOB

Fig.6 shows the characteristics of the flow field with time at different WOB. On the whole, the outlet velocity of the nozzle and the chamber pressure show a trend of increase at 0 s ~ 0.12 s, and decreases at 0.12 s - 0.25 s; when the time is about 0.25 s, the pressure and velocity decrease to 0. With the increase of WOB, the peak velocity in nozzle and peak pressure are increased significantly. The main reason for this phenomenon can be understood since when the WOB increases, the force on the plunger increases and energy used to supercharge the fluid is increased. Furthermore, the increase of the WOB increases the time range of the ultra-high-pressure water jet, furthermore, the increase of the WOB lengthens the holding time of the UHP water jet. The WOB does not affect the plunger motion frequency. In the range of research, the larger WOB is beneficial to the formation of ultra-high-pressure water jet.

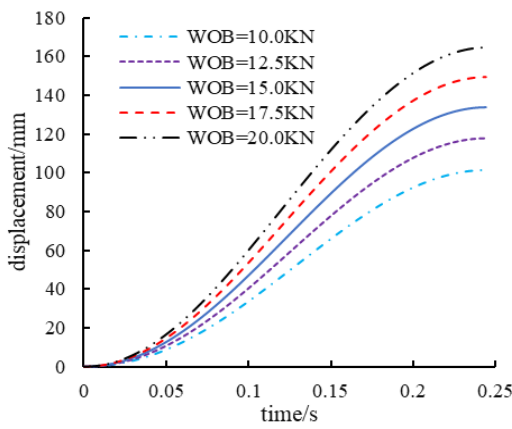
(2) Motion characteristics of plunger

In order to demonstrate the changing tendency of plunger motion with different WOB, the distributions of speed and displacement of plunger are investigated in Fig.7. It is worth noting that with increasing the WOB, the speed and displacement of the plunger tends to increase, and the stroke of the plunger should increase by 6 mm for every 1 kN increase in WOB. The main reason for this phenomenon can be understood since when the WOB increases, the force on the plunger increases and acceleration of the plunger is increased. Therefore, the stroke of plunger to be used for the

intensifier design should be appropriately increased in an actual drilling process when operating at higher WOB.



(a) Speed of plunger



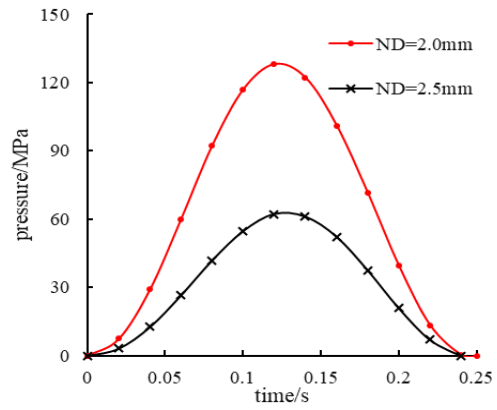
(b) Displacement of plunger

Fig.7 Plunger motion characteristics in different WOB

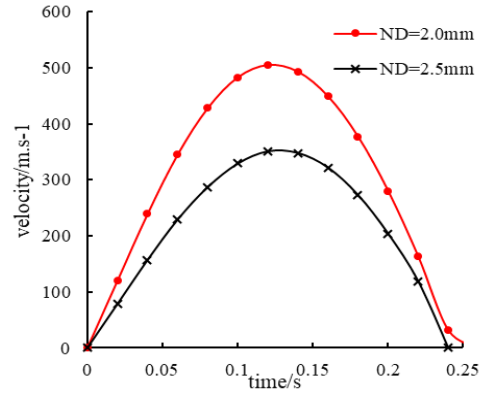
4.3 The effect of nozzle diameter

(1) Characteristic of flow field

Fig. 8 compares the pressurization effect with different nozzle diameter, when the average WOB is 150Kn and pulse WOB is 50kN. It is worth noting that, as the nozzle diameter decreases, the peak pressure and velocity increase, and the formation time of the high-pressure water jet is reduced. Decreasing the nozzle diameter prolongs the holding time of the high-pressure water jet above a certain threshold value, and the decrease of nozzle diameter makes the pressurization period decrease. In the range of diameters investigated in this research, the smaller nozzle diameter is beneficial to the formation of an ultra-high-pressure water jet.



(a) Pressure of UHP water jet

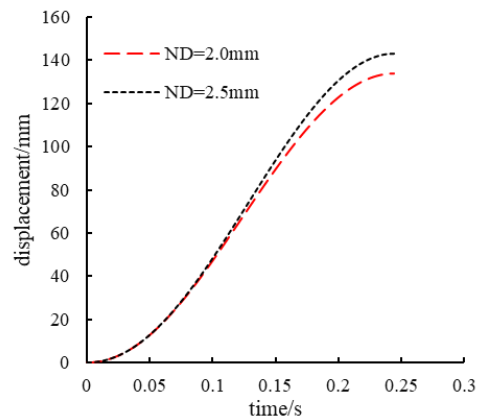


(b) Velocity of UHP water jet

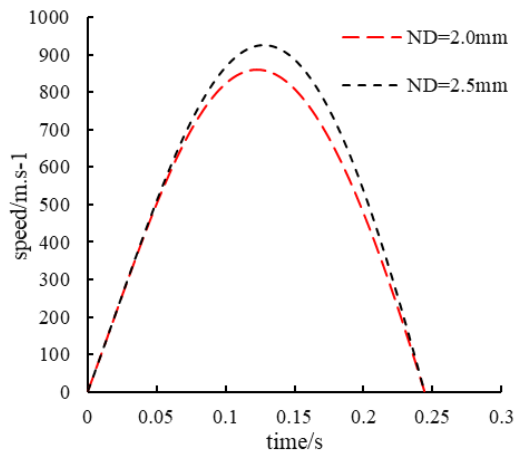
Fig.8 Characteristic of flow field in different nozzle diameter

(2) Motion characteristics of plunger

Fig.9 plots the distribution of speed and displacement of the plunger with different nozzle diameter. It is worth noting that by increasing the diameter of nozzle, the speed and displacement of the plunger tends to increase. Before 0.07 s, the diameter of the nozzle has little effect on the velocity and displacement of the plunger. However, after 0.07 s, with increasing the diameter of the nozzle, the velocity and displacement of the plunger increase more slowly, because the increasing the speed of plunger makes the internal pressure increase and counteract part of WOB, thus reducing the acceleration of the plunger. In terms of displacement, the increase in nozzle diameter increases the stroke of the plunger.



(a) Speed of plunger



(b) Displacement of plunger

Fig.9 Plunger motion characteristics in different frequency

5. CONCLUSIONS

The results of the numerical simulation are greatly affected by the choice of turbulence model. The potential core of the Realizable model and RNG $k-\epsilon$ model is basically the same, and the length of potential core is about 7 mm. With the increase of axial distance, the velocity attenuation of Standard $k-\epsilon$ turbulence model is most noticeable. The RNG $k-\epsilon$ model delivers the maximum impinging pressure, while the Standard model has the minimum; this is consistent with the velocity attenuation characteristics. The RNG $k-\epsilon$ model is used as the turbulence model for jet simulation because of its higher simulation accuracy.

With the increase of WOB, the peak nozzle velocity and peak pressure are increased significantly, which also increases the time range of the ultra-high-pressure water jet. Furthermore, the increase of the WOB lengthens the holding time of the UHP water jet. The WOB does not affect the plunger motion frequency. By increasing the WOB, the speed and displacement of the plunger tends to increase. Therefore, the stroke of plunger allowed in the intensifier design should be appropriately increased in an actual drilling process when operating at higher WOB.

Decreasing the nozzle diameter prolongs the holding time of the high-pressure water jet above a certain threshold value, and the decrease of nozzle diameter makes the pressurization period decrease. Before 0.07 s, the diameter of the nozzle has little effect on the velocity and displacement of the plunger. However, after 0.07 s, with increasing the diameter of the nozzle, the velocity and displacement of the plunger increase slowly. In the range of diameters investigated in this research, the smaller nozzle diameter is beneficial to the formation of an ultra-high-pressure water jet.

Although the behavior of the vibration-activated intensifiers remains difficult to predict due to the nondeterministic nature of the drilling vibration process, it is hoped that the results of this parametric study could help in the optimization of the design of such intensifier technology.

REFERENCES

Teke O, EL Yaşar. Geothermal energy and integrated resource management in Turkey[J]. *Geomechanics and Geophysics for Geenergy and Georesources*, 2018, 4(1):1-10.

Lu Y h, Wang S Y, Chen M, et al. Experimental Study on Mechanical Properties of Hot Dry Rock [J]. *Chinese Journal of Underground Space and Engineering*, 2020(1):8.

Guan Z C, Liu Y W, Wei W Z, et al. Downhole drill string absorption & hydraulic supercharging device working principle and analysis of speed-increasing effect. *Petroleum drilling techniques*, 2012, 40(2):8-13.

Maurer W, Heilhecker J, Love W. High-Pressure Drilling. *Journal of Petroleum Technology*, 1973, 25(07):851-859.

Liao H L, Li G S. Fluid-structure interaction mechanism of water jet impinging rock with saturated fluid. *Chinese Journal of Rock Mechanics and Engineering*, 2005, 24(15):2697-2703.

Liao H, Guan Z, Shi Y, et al. Field tests and applicability of downhole pressurized jet assisted drilling techniques. *International Journal of Rock Mechanics and Mining Sciences*, 2015, 75:140-146.

Wang D, He D. Power Analysis of Downhole Static Pressure Unit. *Journal of southwest-china petroleum institute*, 1995, 17(1):115-120.

Wang D. Study of Downhole Pressure Unit Construction. *Journal of southwest-china petroleum institute*, 1995, 17(3):103-113.

Ai C, Zhou R X, Wang Z X, et al. Whole structural design of the diaphragm pressure converter used in bottomhole. *Journal of Daqing Petroleum Institute*, 2001, 25:92-94.

Sun W, Sun F, Zhao C. Systematic design for a downhole centrifugal supercharging device. *China Petroleum Machinery*, 2006, 34:36-38.

Zhao J, B Y J, Sun P, et al. Design of Downhole Supercharger of Double Helical Slots Driven by Screw Motor. *Oil Field Equipment*, 2010, 39(12): 34-37.

Xu Y, Zhou C, Liu Y et al. Principle and design of screw downhole supercharger. *Drilling & Production Technology*, 2011,34(3):71-74

Wang Z M, Xue L. Hydraulic parameter model for design of fluidics downhole boost compressor. *Acta Petrolei Sinica*, 2008, 29(2):308-312.

Xue L, Wang Z M, Li B G. Structural design of the second-generation downhole jet boost compressor. *China Petroleum Machinery*, 2010, 38(8):24-27.

Xue L, Li B, Wang Z, et al. Ultrahigh-Pressure-Jet-Assisted Drilling Technique: Theory and Experiment. *Journal of Canadian Petroleum Technology*, 2012, 51(4):276-282.

Guan Z, Zhang H, Zhang W, et al. Equipment and technique for improving penetration rate by the transformation of drill string vibration to hydraulic

Hualin Liao, Huajian Wang, John-Paul Latham et al.

pulsating jet[J]. *Petroleum Exploration & Development*, 2014, 41(5):678-683.

Acknowledgements (optional)

This paper acknowledges the support of the National Key Research and Development Program of China (2021YFE0111400), and the Horizon programme of the EU's funding of the ORCHYD project, EU-H2020(101006752-ORCHYD).